INSTITUTE OF PHYSICS PUBLISHING MEASUREMENT SCIENCE AND TECHNOLOGY
Meas. Sci. Technol. 15 (2004) 2406–2411 PII: S0957-0233(04)84803-3

Displacement measuring technique for satellite-to-satellite laser interferometer to determine Earth's gravity field

Shigeo Nagano[1], Taizoh Yoshino[1,4], Hiroo Kunimori[1], Mizuhiko Hosokawa[1], Seiji Kawamura[2], Takashi Sato[3] and Masashi Ohkawa[3]

[1] National Institute of Information and Communications Technology, Koganei, Tokyo 184-8795, Japan
[2] National Astronomical Observatory of Japan, Mitaka, Tokyo 181-8588, Japan
[3] Faculty of Engineering, Niigata University, Ikarashi, Niigata 950-2181, Japan

E-mail: nagano@nict.go.jp

Received 11 August 2004, in final form 23 September 2004
Published 19 November 2004
Online at stacks.iop.org/MST/15/2406
doi:10.1088/0957-0233/15/12/009

Abstract
We present a new displacement measuring technique with simplicity, robustness, high sensitivity and wide measurement range. A set of a frequency shifter and a voltage–frequency converter is used to lock a homodyne interferometer on the half-bright fringe by eliminating the Doppler fringe resulting from mirror motion. The mirror displacement is directly retrieved from the feedback signal of a fringe control loop. By developing a table-top interferometer, we successfully demonstrated signal recovery without significant degradation. The achieved displacement sensitivity and measurement range of the interferometer were 24 nm $Hz^{-1/2}$ and 1.3 mm at a Fourier frequency of 0.1 Hz, respectively. This technique was found to have a potential for application to precise displacement measurements. It is, in particular, suitable for a satellite-to-satellite laser interferometer to determine Earth's gravity field.

Keywords: laser interferometer, displacement measurement, satellite-to-satellite laser interferometer, satellite gravity mission

1. Introduction

Laser interferometers are widely used in precise displacement measurements from less than nanometre to the metre scale. Many interferometric measurements for engineering, metrology, lithography and advanced scientific applications require high displacement sensitivity and wide measurement range (Charette *et al* 1992, Halverson and Spero 2002, LISA Study Team 2000). The Earth's gravity field determination using a satellite-to-satellite laser interferometer (SSI) is one such application.

The satellite gravity mission aims to map Earth's global gravity field and to monitor its temporal variations. The mission's principle is to observe the free-fall motion of a satellite in the gravity field; the satellite is continuously tracked by a global positioning system, and a non-gravitational force acting on it has to be separated from the signal by accelerometers (Seeber 2003). The gravity recovery and climate experiment (GRACE) was launched to resolve the gravity field with an accuracy of 1 cm and a spatial resolution of 500 km by measuring the relative motion between twin satellites with a microwave-ranging system (GRACE Team 1998). However, further information on the gravity field is requested to expand our knowledge concerning Earth's system. A satellite gravity mission is proposed in Japan

[4] Present address: Mitsubishi Electric Corporation, Kamakura, Kanagawa 247-8520, Japan.

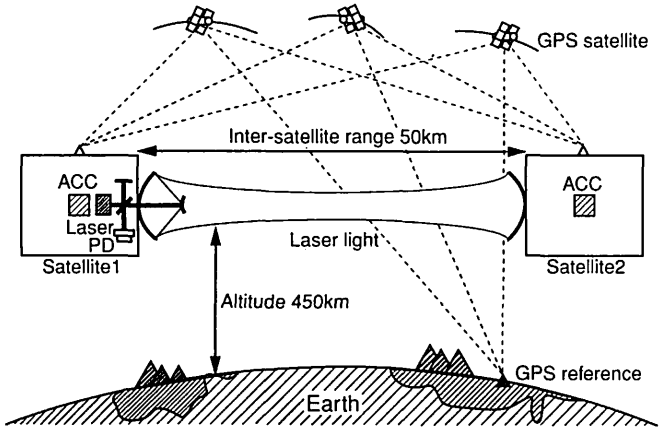

Figure 1. The concept of the satellite gravity mission proposed in Japan. Twin satellites will be launched into a near-polar orbit of 450 km altitude and fly 50 km apart. The satellites are tracked by a global positioning system (GPS) and the non-gravitational forces acting on them are measured with precision accelerometers (ACCs). A laser interferometer is employed to detect the relative motion between the satellites. A laser and photodiode (PD) are contained in a lead satellite 1. The laser beam emitted from satellite 1 is directly reflected by following satellite 2.

(Fukuda *et al* 2003). The mission goal is to detect changes in the geoid with millimetre-level accuracy and shorter spatial resolution of 100 km. The mission concept is illustrated in figure 1. An SSI will be employed to measure the relative velocity change of $10\,\mathrm{nm\,s^{-1}}$ between two satellites in a measurement band from 10^{-2} Hz to 1 Hz. The maximum relative velocity of the satellites is predicted to be $10\,\mathrm{cm\,s^{-1}}$ in low Earth orbit with an eccentricity of 1.6×10^{-3} (Otsubo 2002). Thus, interferometric displacement measurement with a wide measurement range and high sensitivity in the low-frequency band is one of the key technologies to attain the mission goal.

The laser interferometers available for the SSI can be classified into heterodyne and homodyne interferometers by their frequencies (Bobroff 1993). The heterodyne interferometer uses beams with two different frequencies for each arm of the interferometer. The displacement signal is proportional to the phase change of the interference fringe and is extracted after the demodulation process by the heterodyne frequency. Traditional and commercial interferometers have utilized a two-mode Zeeman-stabilized He–Ne laser, which has two co-propagating beams with orthogonal polarizations separated in frequency by a few MHz (Tanaka and Nakamura 1983, Bobroff 1987, Sutton 1987). Acousto-optic modulators were also employed in many experiments instead of the two-mode laser to generate the frequency difference in two beams (Tanaka *et al* 1989, Jennrich *et al* 2001, Lawall and Kessker 2000). These demonstrations have shown the potential to measure displacement with over nanometre-level accuracy and wide measurement range, regardless of the periodic errors attributed to the inevitable mixing of polarization and frequency due to imperfect polarizing optics, scattered light and other factors (Wu *et al* 1999, Lawall and Kessker 2000). Heterodyne interferometers, however, could have difficulties to be applied to the SSI for the following practical reason. Complex electronics related to demodulation for signal extraction must be loaded into the satellite, although

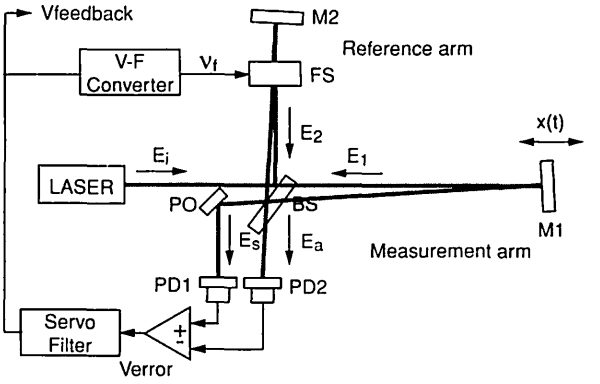

Figure 2. Conceptual design of a differential displacement measurement using an interferometer with a set of a frequency shifter and a voltage–frequency converter. E: light field, V: voltage, ν_f: carrier frequency, x: displacement, BS: beamsplitter, M: mirror, PO: pick-off plate, PD: photodiode, FS: frequency-shifter and V–F converter: voltage–frequency converter.

simple and small electronics are required for the satellite gravity mission we plan.

On the other hand, the homodyne interferometer uses one laser frequency for both arms of the interferometer. The displacement signal is directly proportional to the interference fringe, and thus simple electronics for the signal extraction is allowed because of no demodulation process. This is particularly important for the satellite gravity mission. However, there also exist periodic errors in this interferometer, which are caused by optical mixing according to previous studies (Augustyn and Davis 1990, Wu and Su 1996).

In this paper, we present a new technique for displacement measurement using a homodyne interferometer with a set of a frequency shifter and a voltage–frequency converter. It has several features: simplicity, robustness, wide measurement range and high sensitivity. Additionally it is, in principle, free of periodic errors. A laser interferometer, which was explicitly designed to simulate the gravity field retrieval of the SSI on the ground, was employed for the demonstration of the displacement measurement. From the demonstration, our technique was found to be available for accurate displacement measurement in diverse fields. It is especially suitable for the SSI to be employed in future satellite gravity missions.

2. Principle

The conceptual design of a laser interferometer for differential displacement measurement we propose is illustrated in figure 2. It is based on a Michelson interferometer with a frequency shifter driven by a voltage–frequency converter. We used a Michelson interferometer in this analysis, but it is applicable to any two-beam interferometer. The perpendicular and in-line arms of the interferometer serve as the reference and measurement arms, respectively. Polarization-insensitive optical components were employed in conjunction with the laser beams in both arms, consequently free of periodic errors in principle. The velocity of the mirror (M 1) is the time derivative of the mirror displacement $x(t)$ and given by $u(t) = \mathrm{d}x(t)/\mathrm{d}t$. The frequency of the measurement beam is shifted by $2\nu_0 u(t)/c$ due to the Doppler effect, where ν_0 and c are the laser frequency and speed of light, respectively. Therefore,

the mirror displacement can be obtained immediately if the Doppler frequency is correctly measured.

The frequency shifter driven with a carrier frequency of ν_f can generate an artificial frequency shift in the reference beam by $2\nu_f$ using it in double-pass. The field amplitude returning from each arm is

$$E_1 = t_{BS}\, r_1 E_0 \exp\left\{i\omega_0(t - 2L_1/c) + i4\pi \int dt\, \nu_0 u(t)/c\right\}$$

$$= t_{BS}\, r_1 E_0 \exp\left\{i\omega_0(t - 2L_1/c) + i4\pi \int \nu_d\, dt\right\}, \qquad (1)$$

$$E_2 = i r_{BS} r_2 E_0 \exp\left\{i\omega_0(t - 2L_2/c) + i4\pi \int \nu_f\, dt\right\}, \qquad (2)$$

where r and t represent the amplitude reflectivity and transmissivity, and subscripts 1, 2 and BS indicate the M1, M2 and beamsplitter. $\omega_0/2\pi$ is the optical frequency. L_1 and L_2 are the static lengths of the measurement and reference arms, respectively. We defined $\nu_0 u(t)/c$ as ν_d in equation (1). These field amplitudes are recombined at the beamsplitter and produce an interference pattern on the photodiodes placed at the symmetric and antisymmetric ports of the interferometer (PD1 and PD2). The photocurrent on each PD is written as

$$I_s = \frac{I_0}{2}\left[1 - \cos\left\{\frac{2\omega_0(L_2 - L_1)}{c} + 4\pi \int dt(\nu_d - \nu_f)\right\}\right], \qquad (3)$$

$$I_a = \frac{I_0}{2}\left[1 + \cos\left\{\frac{2\omega_0(L_2 - L_1)}{c} + 4\pi \int dt(\nu_d - \nu_f)\right\}\right], \qquad (4)$$

where we assumed $r_1 = r_2 = 1$ and $r_{BS} = t_{BS} = 1/\sqrt{2}$. The incident power into the interferometer is written as $I_0 = |E_0|^2$. The quantum efficiency of the PDs was assumed to be unity for convenience. Balanced detection, which subtracts the output of one PD from that of the other, can enhance the signal-to-noise ratio and suppress the laser intensity noise by common-mode rejection. The output of a subtractor (a triangle with '+' and '−' input) is given by

$$V_{error} \propto I_0 \cos\left\{\frac{2\omega_0(L_2 - L_1)}{c} + 4\pi \int dt(\nu_d - \nu_f)\right\}. \qquad (5)$$

Equation (5) yields the ac components of the interference fringe. Since the first term in the cosine represents the static phase and can be chosen at $\pi/2$, the time evolution of the fringe is proportional to the integration of the frequency difference between two beams from each arm of the interferometer. If the carrier frequency ν_f is tuned to be exactly equal to the Doppler frequency ν_d by a feedback control loop, V_{error} is maintained at the zero point. The interferometer is locked at the half-bright fringe. The mirror displacement can be obtained by monitoring the feedback signal to the voltage–frequency converter.

The block diagram of the feedback control loop is shown in figure 3, where E and H represent the frequency response of a servo filter and that of a voltage–frequency converter, respectively. I denotes the frequency response for signal detection. $1/s$ converts frequency modulation to phase modulation, where s is the Laplace frequency variable. From figure 3, the feedback voltage to the voltage–frequency converter is expressed as

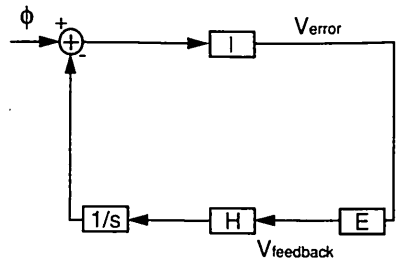

Figure 3. Block diagram of feedback control loop. I represents the frequency response for signal detection. E and H are the frequency response of a servo filter and that of a voltage–frequency converter, respectively. s denotes the Laplace frequency variable and ϕ is the integration of Doppler frequency caused by mirror motion.

$$V_{feedback} = \frac{IE\dot{\phi}}{1 + IEH(1/s)} = \frac{IE(2\nu_d/s)}{1 + IEH(1/s)} \qquad (6)$$

$$\simeq \frac{2\nu_d}{H}, \qquad (|IEH(1/s)| \gg 1), \qquad (7)$$

where ϕ represents the integration of the Doppler frequency, and it can be written as $2\nu_d/s$ in the frequency domain. If the open-loop gain of the control loop is much larger than unity, the Doppler frequency, proportional to the mirror velocity, can be obtained more easily by directly reading out the feedback signal. H usually has a flat frequency response in the frequency band that we are interested in.

The measurement range of the interferometer would be practically restricted by the output frequency range of the voltage–frequency converter rather than the dynamic range of the frequency shifter. In such a case, the Doppler frequency corresponding to the velocity of the moving mirror should not exceed the output frequency range to maintain the interferometer operation.

3. Experimental setup

The laser interferometer we set up has two purposes: one is to demonstrate our measuring technique experimentally and the other is to apply it to a table-top instrument available to simulate the gravity field recovery of the SSI on the ground. The interferometer is explicitly designed for application to the ground simulator. In the satellite gravity mission conceived in Japan, the SSI is required to measure the relative velocity change of $10\,\mathrm{nm\,s^{-1}}$ between two satellites in the measurement band from 10^{-2} to 1 Hz. This corresponds to a displacement sensitivity of $1.6/f\,\mathrm{nm\,Hz^{-1/2}}$, where f is the Fourier frequency. Therefore, it was set as a primary goal for the experimental demonstration. The measurement range needed for the SSI simulation will be satisfied in the next development phase, and it is out of scope of this work.

3.1. Interferometer with frequency shifters

The experimental setup of the laser interferometer for displacement measurement is shown in figure 4. We employed a modified Mach–Zehnder laser interferometer. The light source is a laser-diode-pumped monolithic Nd:YAG laser emitting 200 mW in optical power at a wavelength of

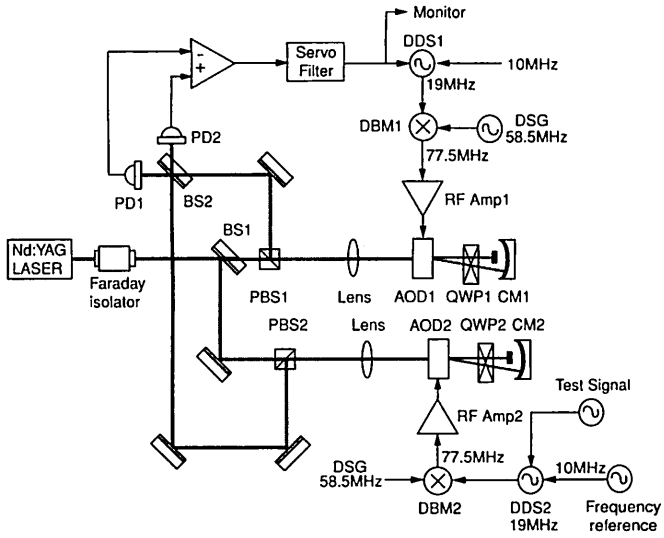

Figure 4. Schematic diagram of the Mach–Zehnder interferometer for differential displacement measurement. BS: beamsplitter, CM: concave mirror, QWP: quarter waveplate, PD: photodiode, AOD: acousto-optic deflector, DDS: direct digital synthesizer, DSG: digital signal generator and DBM: double-balanced mixer.

1064 nm (InnoLight, Mephisto 200NE). It oscillates at a single frequency, TEM_{00}-mode with linear polarization. The laser is a reasonable choice considering its low intrinsic noise.

A p-polarized laser beam through a Faraday isolator is divided by a beamsplitter (BS 1) into an in-line and a perpendicular arm. The in-line arm serves as a reference arm, in which a frequency shifter tunes the laser frequency to lock the interferometer at the half-bright fringe. The perpendicular arm is a measurement arm. Another frequency shifter is equipped as a simulation signal generator. It produces the pseudo-Doppler shift to simulate the SSI in Earth's gravity field; the mirror displacement required for the SSI simulation is not practical if a mechanically moving mirror is employed. This arm is constructed parallel to the in-line arm to reduce common-mode noise resulting from the environment.

The frequency shifter is composed of an acousto-optic deflector (AOD), a quarter-wave plate and a concave mirror. The laser beam is modulated in frequency by the AOD (Brimrose: TEM-80-2-1064). The resultant changes in diffraction angle by the frequency modulation are cancelled by doubly passing the beam through the AOD in combination with the concave mirror. The concave mirror reflects the beam back to the same optical path by placing it with its centre of curvature from the AOD. The quarter-wave plate flips the polarization of the laser beam from p-polarization to s-polarization so that the laser beam coming back from the frequency shifter is separated from the incident beam by a polarizing beamsplitter.

The laser beams from both arms are superimposed on the BS2, and an interference fringe is formed on two Si-PIN photodiodes (PD1 and PD2).

Typically AODs generate an inevitable Doppler shift in the optical frequency by radio frequency. For dealing with the Doppler frequencies that approach zero, the AOD in the simulation signal generator is also used to shift the optical frequency by the same frequency shifted in the reference arm. An alternative technique is to employ an additional AOD in the frequency shifter, which only cancels the optical frequency shift. Consequently, the frequency modulator in the measurement arm would be removed as shown in figure 2.

3.2. Voltage–frequency converter

The voltage–frequency converter consists of a direct digital synthesizer (DDS), a digital signal generator (DSG) and a double-balanced mixer (DBM). The outputs of the DDS and DSG are up-converted by the DBM to produce a carrier at 77.5 MHz for driving the AOD. The obtained carrier is applied to the AOD after amplification and band-pass filtering. The DSG oscillating at a fixed frequency of 58.5 MHz is commonly used in two voltage–frequency converters (Hewelett Packard: ESG-D4000A). The DDS generator is a key device in the voltage–frequency converter (Digital Signal Technology, FIX-20 SP1). An analogue signal from a 10 bit digital-to-analogue (D/A) converter with a sampling frequency of 50 MHz is low-pass filtered to obtain a sine wave with acceptable distortion. The frequency of the sine wave can be phase-continuously tuned around a centre frequency of 19 MHz by a control voltage applied through a 16 bit analogue-to-digital (A/D) converter. The frequency resolution is set at 11.64 mHz to generate the pseudo-Doppler frequency shift corresponding to a velocity change of $12\,\mathrm{nm\,s^{-1}}$. The output frequency range of 762.839 Hz is restricted by the resolution of the A/D converter. This is insufficient for the simulation of the global Earth's gravity field recovery of the SSI, which needs to produce a Doppler fringe up to 200 kHz at a Fourier frequency of 0.18 mHz. We think, however, there are no obstacles to producing such a frequency shift. An individual DDS generator with a 24 bit $\Delta\Sigma$ A/D converter could be utilized as an auxiliary frequency actuator instead of the DSG generator, and it allows the frequency of the measurement beam to be shifted by more than 390 kHz at 0.18 mHz. The extension of output frequency range will be addressed in the next phase of simulator development.

The DDS generator we employed is designed to update a new frequency within 140 μs and has a phase delay of less than 150° at a Fourier frequency of 1 kHz. This is because the feedback loop for interferometer locking needs a control bandwidth of 1 kHz with a reasonable design for the feedback servo. The residual motion around the locking point results in the degradation of the feedback loop performance. The required feedback gain is more than 200 dB at 0.18 mHz to suppress the residual fluctuation within 1/100 of the laser wavelength.

The phase noise of voltage–frequency converters appears in the simulator output as a spurious signal. Since the DDS generator was a substantial part of the noise owing to poor stability in the internal reference clock, an external clock of 10 MHz from a hydrogen-maser frequency standard was provided to decrease the phase noise.

3.3. Servo electronics

A differential amplifier excludes the influence of the laser intensity noise from the signal detected by the PDs. The signal from the amplifier is appropriately filter-amplified by servo electronics and directed towards the voltage–frequency converter in the in-line arm to control the motion of the fringe

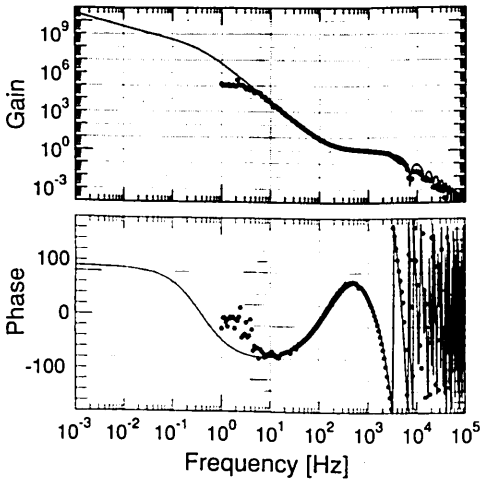

Figure 5. Measured open-loop transfer function of the feedback control system. The bold line and dots represent calculated and measured open-loop transfer functions of the feedback control loop, respectively.

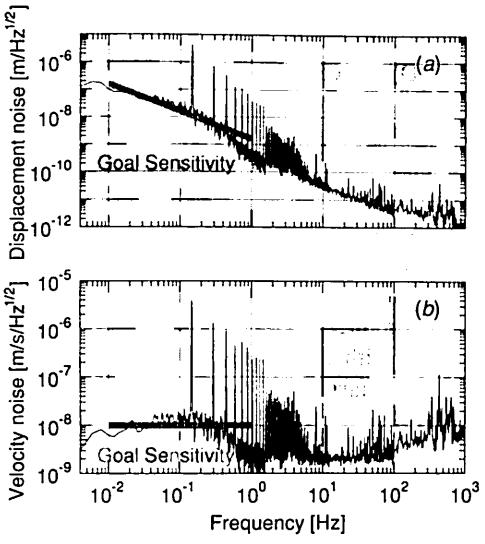

Figure 6. (*a*) Displacement noise spectrum and (*b*) velocity noise spectrum of Mach–Zehnder interferometer. The goal sensitivity of the SSI for a Japanese satellite gravity mission is also indicated by the grey lines.

pattern. The servo electronics were designed considering the low electronic noise performance and the compensation of the phase delay due to the DDS generator.

4. Experimental results

The measured open-loop transfer function of the feedback control system is plotted in figure 5. The control bandwidth was approximately 1 kHz, and the open-loop gain achieved was more than 200 dB below 4 mHz. The control bandwidth is restricted by the sampling frequency of the A/D converter in the DDS 1. The dips in the gain curve at 7.1 kHz and its harmonics originate from the transfer function of A/D conversion.

Figure 6(*a*) shows the displacement noise spectrum of the interferometer estimated from the feedback signal to the voltage–frequency converter. It will provide the limitation of the displacement signal retrieval. The displacement noise level is below $2.4/f$ nm $Hz^{-1/2}$ between 10^{-2} Hz and 1 Hz. The laser power on each PD was about 12 mW after attenuation using a neutral density filter. The shot noise level corresponding to the photocurrent was calculated to be 1.4×10^{-15} m $Hz^{-1/2}$. The velocity noise spectrum is also shown in figure 6(*b*). The measured noise level of 15 nm $s^{1/2}$ $Hz^{1/2}$ is no significant level to detect changes in the geoid with millimetre-level accuracy.

The present displacement noise level is not intrinsic to the displacement measuring technique. The displacement noise below 0.1 Hz was dominated by the phase noise of the DDS generator in the voltage–frequency converter. It was revealed from a calibrated error signal of a phase noise measurement, in which one DDS generator is phase locked to the other with a phase-locked loop. The peak at 0.14 Hz and its harmonics in the noise spectra were also found to be caused by the generator. They will be removed by replacement with DDS generators with lower phase noise. The air density variations propagating to the optical components influenced the displacement measurement between 0.1 Hz and 1 Hz, since the interferometer was constructed on an optical table in air without special isolation for such noise. It should be noted that any optical path length fluctuations inside the AOD in the reference arm will be indistinguishable from the signal. The optical path length fluctuation δL caused by the temperature fluctuation of the AOD is given by $\delta L = 2L(\mathrm{d}n/\mathrm{d}t)\delta T$, where L is the length of the AOD crystal, $\mathrm{d}n/\mathrm{d}T$ represents the temperature coefficient of refractive index of the crystal and δT is the temperature fluctuation. For the properties of tellurium dioxide (TeO_2) used for the AOD, the corresponding displacement noise level was estimated to be below 8 nm $Hz^{-1/2}$ at 0.1 Hz with the measured temperature fluctuation of less than 20 mK $Hz^{-1/2}$. This noise level is still lower than the present sensitivity of the interferometer.

For the evaluation of the performance of our interferometer, we measured the residual spectrum of the displacement signal reconstructed in the feedback signal with respect to the simulation signal applied to the signal generator. We electrically subtracted the simulation signal from the feedback signal during the simulated signal injection. The injected signal was a synthesized sine wave swept from 4×10^{-3} Hz to 1 Hz in 2500 s and its amplitude was predetermined to be about 10^{-6} m $Hz^{-1/2}$ in displacement at 10 mHz, which is equivalent to the expected change in the inter-satellite range caused by variations in the gravity field (Kim 2000). In figure 7, the solid and dotted lines indicate the residual spectrum and the feedback signal spectrum during the injection of the simulation signal, respectively. The displacement noise spectrum of the interferometer has also been shown by the dashed line for comparison. The residual spectrum and the displacement noise spectrum are in good agreement. Therefore, it was found that the simulation signal was successfully reconstructed in the feedback signal without significant degradation. Our interferometer is not a polarization interferometer, and thus free of periodic errors in principle. Periodic errors were not observed at the current sensitivity level.

The present measurement range was limited by the output frequency range of the voltage–frequency converter for controlling the motion of the interference fringe. The

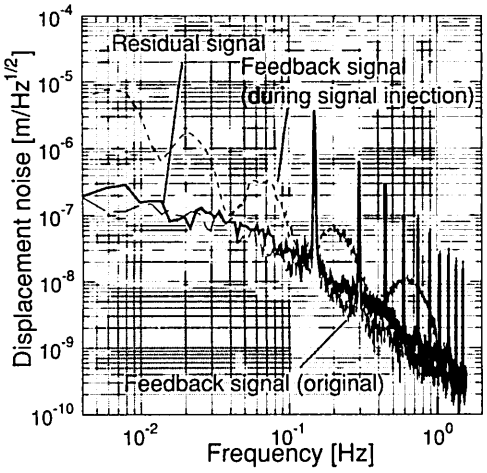

Figure 7. Residual spectrum of retrieved displacement signal. The solid and dotted lines are the residual spectrum and the feedback signal spectrum to the frequency shifter, respectively. The dashed line indicates the displacement noise spectrum of the Mach–Zehnder interferometer.

obtainable frequency shift on the reference beam is about 1.5 kHz, which corresponds to 0.8 mm s^{-1} in allowable mirror velocity. Any mirror motion within this velocity range can be measured with the achieved sensitivity. The measurement range in displacement is estimated to be $129/f$ μm.

The lock acquisition of the interferometer had no difficulties, even if a high frequency Doppler fringe appeared in the interferometer output. The interferometer could be locked immediately after feeding back the control signal to the voltage–frequency converter. The long-term reliability of the interferometer was tested simultaneously with the sensitivity measurement. There was no significant degradation in the sensitivity during the long-term operation of the interferometer over several hours.

5. Conclusion

We have presented a new technique for displacement measurement using a laser interferometer with a set of a frequency shifter and a voltage–frequency converter. It has simplicity, robustness, high sensitivity and wide measurement range. Additionally, it is free of periodic errors in principle. A Mach–Zehnder interferometer with one AOD for each arm, which was designed to simulate Earth's gravity field recovery of the SSI, was used for the demonstration of the measuring technique. The displacement noise level achieved was below $2.4/f$ nm $Hz^{-1/2}$ from 10^{-2} Hz to 1 Hz. The measurement range was $129/f$ μm, which was limited by the output frequency range of the voltage–frequency converter. The spectrum measurement of the residuals between the simulation and the retrieved signal revealed that our technique can be used to precisely measure displacement in various applications. It is particularly suitable for future satellite gravity missions following GRACE, in which SSI will be employed to improve the accuracy and spatial resolution of the gravity field. The constructed interferometer is now being applied to the development of a ground simulator that will be used to demonstrate the gravity field retrieval with unprecedented accuracy from the pseudo-Doppler shift corresponding to the relative motion of twin satellite in the gravity field. The ground simulator will be valuable to study the feasibility of the SSI in future missions.

Acknowledgments

The authors would like to thank I Naito for his efforts to start this project. This work was supported by Special Coordination Funds for Promoting Science and Technology from the Ministry of Education, Culture, Sports, Science and Technology in Japan.

References

Augustyn W and Davis P 1990 An analysis of polarization mixing errors in distance measuring interferometers *J. Vac. Sci. Technol.* B **8** 2032–6

Bobroff N 1987 Residual errors in laser interferometry from air turbulence and nonlinearity *Appl. Opt.* **26** 2676–82

Bobroff N 1993 Recent advances in displacement measuring interferometry *Meas. Sci. Technol.* **4** 907–26

Charette P G, Hunter I W and Brenan C J H 1992 A complete high performance heterodyne interferometer transducer for microactuator control *Rev. Sci. Instrum.* **63** 241–8

Fukuda Y, Otsubo T, Yoshino T and Okubo S 2003 A new project of gravity mission studies in Japan Presented at *IUGG2003 (Sapporo, Japan)*

GRACE Team 1998 *GRACE Science and Mission Requirements Document (SMRD)* GRACE327-200 JPL D-15928

Halverson P G and Spero R E 2002 Signal processing and testing of displacement metrology gauges with picometre-scale cyclic nonlinearity *J. Opt. A: Pure Appl. Opt.* **4** S304–10

Jennrich O, Stebbins R T, Bender P L and Pollack S 2001 Demonstration of the LISA phase measurement principle *Class. Quantum Grav.* **18** 4159–64

Kim J 2000 Simulation study of a low–low satellite-to-satellite tracking mission *PhD Thesis* University of Texas

Lawall J and Kessker E 2000 Michelson interferometry with 10 pm accuracy *Rev. Sci. Instrum.* **71** 2669–76

LISA Study Team 2000 *LISA Laser Interferometric Space Antenna: A Cornerstone Mission for the Observation of Gravitational Waves* European Space Agency ESA-SCI(2000)11

Otsubo T 2002 Private communication

Seeber G 2003 *Satellite Geodesy* 2nd edn (Berlin: de Gruyter)

Sutton C M 1987 Non-linearity in length measurement using heterodyne laser Michelson interferometry *J. Phys. E: Sci. Instrum.* **20** 1290–2

Tanaka M and Nakamura K 1983 A new optical interferometer for absolute measurement of linear displacement in the subnanometer range *Japan. J. Appl. Phys.* **22** 233–5

Tanaka M, Yamagami T and Nakamura K 1989 Linear interpolation of periodic error in a heterodyne laser interferometer at subnanometer levels *IEEE Trans. Instrum. Meas.* **38** 552–4

Wu C M, Lawall J and Deslattes R D 1999 Heterodyne interferometer with subatomic periodic nonlinearity *Appl. Opt.* **38** 4089–94

Wu C M and Su C S 1996 Nonlinearity in measurements of length by optical interferometry *Meas. Sci. Technol.* **7** 62–8